Cardiol Ther (2023) 12:85–99
https://doi.org/10.1007/s40119-022-00295-1

REVIEW

Emerging PET Tracers in Cardiac Molecular Imaging

Shashi Bhushan Singh · Sze Jia Ng · Hui Chong Lau · Kishor Khanal · Sanket Bhattarai · Pranita Paudyal · Bimash Babu Shrestha · Rizwan Naseer · Simran Sandhu · Saket Gokhale · William Y. Raynor

Received: October 12, 2022 / Accepted: November 26, 2022 / Published online: January 3, 2023

ABSTRACT

^{18}F-fluorodeoxyglucose (FDG) and ^{18}F-sodium fluoride (NaF) represent emerging PET tracers used to assess atherosclerosis-related inflammation and molecular calcification, respectively. By localizing to sites with high glucose utilization, FDG has been used to assess myocardial viability for decades, and its role in evaluating cardiac sarcoidosis has come to represent a major application. In addition to determining late-stage changes such as loss of perfusion or viability, by targeting mechanisms present in atherosclerosis, PET-based techniques have the ability to characterize atherogenesis in the early stages to guide intervention. Although it was once thought that FDG would be a reliable indicator of ongoing plaque formation, micro-calcification as portrayed by NaF-PET/CT appears to be a superior method of monitoring disease progression. PET imaging with NaF has the additional advantage of being able to determine abnormal uptake due to coronary artery disease, which is obscured by physiologic myocardial activity on FDG-PET/CT. In this review, we discuss the evolving roles of FDG, NaF, and other PET tracers in cardiac molecular imaging.

Shashi Bhushan Singh and Sze Jia Ng contributed equally to this work.

S. B. Singh · K. Khanal · B. B. Shrestha · S. Gokhale · W. Y. Raynor
Department of Radiology, Hospital of the University of Pennsylvania, 3400 Spruce Street, Philadelphia, PA 19104, USA

S. J. Ng · H. C. Lau · R. Naseer
Department of Medicine, Crozer-Chester Medical Center, 1 Medical Center Boulevard, Upland, PA 19013, USA

K. Khanal
Division of Cardiology, Memorial Healthcare System, 3501 Johnson Street, Hollywood, FL 33021, USA

S. Bhattarai
Department of Medicine, KIST Medical College, Mahalaxmi 01, Lalitpur, Bagmati, Nepal

P. Paudyal
West China Hospital, Sichuan University, 37 Guoxue Lane, Wuhou District, Chengdu 610041, Sichuan, China

S. Sandhu
College of Health and Human Development, Pennsylvania State University, 10 East College Avenue, University Park, PA 16802, USA

W. Y. Raynor
Department of Radiology, Rutgers Robert Wood Johnson Medical School, 1 Robert Wood Johnson Place, MEB #404, New Brunswick, NJ 08901, USA

Keywords: FDG; NaF; ^{18}F-flurpiridaz; ^{18}F-flubrobenguane; PET/CT; PET/MRI; Atherosclerosis; Perfusion; Sarcoidosis; Amyloidosis

Key Summary Points

Early diagnosis of atherosclerosis is a clinical necessity in order to allow for timely intervention before irreversible changes have taken place.

^{18}F-fluorodeoxyglucose (FDG) is a PET tracer with many uses and was first described as a marker of vascular inflammation associated with atherosclerosis over 20 years ago.

More recently, PET imaging with ^{18}F-sodium fluoride (NaF) has gained attention for the purpose of imaging vascular micro-calcification, which is a component of atheroma progression.

Although both FDG and NaF both appear promising for the assessment of atherogenesis, the close association between NaF uptake and established cardiovascular risk factors as well as increased specificity of NaF uptake allowing for visualization of coronary artery involvement suggest that NaF may be the optimal PET tracer for atherosclerosis imaging.

INTRODUCTION

The 2020 American Heart Association (AHA) statistical update reported that cardiovascular diseases (CVD) are attributed to more than 1000 deaths daily worldwide [1]. Atherosclerosis, a multi-factorial and progressive process, is a major cause of CVD and related complications, including stroke and peripheral vascular disease [1]. Medical and lifestyle interventions are only effective at reversing disease until a certain point; therefore, it is of utmost importance to detect atherosclerosis in the early stages.

The development of atherosclerosis usually begins with endothelial cell dysfunction, triggered by underlying cardiovascular risk factors including hyperlipidemia, aging, hypertension, or diabetes. This is followed by accumulation of proinflammatory cells and fatty streak formation [2]. Later, molecular micro-calcification of atheromatous plaque forms and progresses into structural macro-calcification, gradually leading to high risk of plaque rupture and vessel occlusion [3]. In the past, numerous conventional imaging techniques have been used in identifying macro-calcification, including cardiac magnetic resonance imaging (CMR), coronary computed tomographic angiography (CTA), intravascular ultrasonography, optical coherence tomography, and coronary artery calcium score (CACS) via CT; however, none of these modalities demonstrate the ability to detect micro-calcification in the early stages of the disease [1, 4].

Molecular imaging with positron emission tomography (PET), more common in the clinical setting as the hybrid modality PET/computed tomography (CT), is capable of detecting early-stage disease by identifying specific changes in metabolism [5]. To date, ^{18}F-fluorodeoxyglucose (FDG) and ^{18}F-sodium fluoride (NaF) are among the two most widely studied PET tracers in atherosclerosis imaging (Fig. 1) [6–8]. In addition, many other tracers are in current use within cardiac molecular imaging [9]. We aim to review the properties and clinical applications of emerging PET radiotracers in nuclear cardiology, with an emphasis on early detection of atherosclerosis with FDG and NaF. This article is based on previously conducted studies and does not contain any new studies with human participants or animals performed by any of the authors.

^{18}F-FLUORODEOXYGLUCOSE (FDG)

Myocardial Injury and Inflammation

Myocardial tissue primarily utilizes fatty acids as source of energy, but under ischemic conditions, myocardial cells consume glucose as their

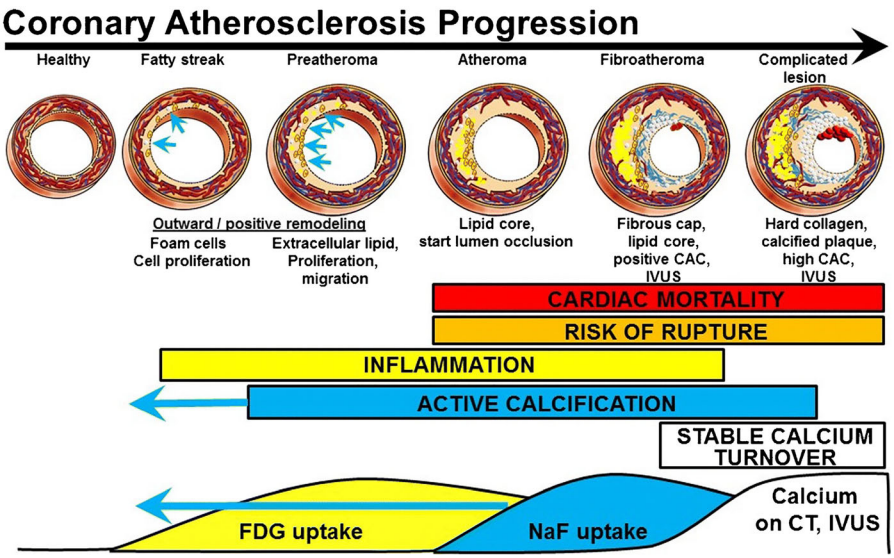

Fig. 1 The development of a complicated atheromatous plaque with hypothesized changes visible by imaging. Although it is established that NaF uptake precedes coronary artery calcium (CAC) visible on CT, new data suggest that NaF uptake may be present earlier relative to inflammation portrayed by FDG than previously thought (*blue arrows*). Image reprinted without changes from McKenney-Drake et al. [8] under the Creative Commons Attribution 4.0 International License (CC BY). https://creativecommons.org/licenses/by/4.0/

primary energy source. Cardiomyocytes with diminished blood supply can undergo an irreversible pattern of infarction and scar tissue formation with total loss of contractile abilities or can bear the stress with temporary, reversible stunning with loss of contractile properties, which is considered hibernating myocardium [10].

As the most widely used PET tracer with major applications in oncology, neurology, infection, and inflammation, FDG serves as a glucose analog and becomes trapped within cells that demonstrate a high rate of glycolysis [11]. This occurs when FDG is converted to FDG-6-phosphate by hexokinase, accumulating intracellularly without being further metabolized. Since the 1980s, FDG has been used to characterize myocardial viability in patients with coronary artery disease [12]. Clinically, FDG cardiac imaging is routinely performed in combination with myocardial perfusion imaging using either positron-emitting or single photon-emitting radiotracers. Ischemic cardiomyopathy can be associated with either myocardial scar or hibernating myocardium. Preserved myocardial perfusion and viability are seen in healthy tissue, whereas both are reduced in non-viable areas of myocardium. A region with preserved (or elevated) FDG uptake but reduced myocardial perfusion indicates viable hibernating myocardium, which can be treated by vascular intervention [13].

FDG uptake in the myocardium has also been used to assess for cardiac sarcoidosis, where it was found to be superior to perfusion single-photon emission computed tomography (SPECT) and delayed enhanced CMR to not only diagnose but also monitor therapeutic responses [14]. Methods of suppressing physiologic myocardial glucose uptake prior to FDG-PET imaging have become a standard practice to facilitate identification of abnormal activity. Specifically, low-carbohydrate and ketogenic dietary protocols have been shown to improve detection of cardiac sarcoidosis [15–17]. Further metabolism suppression can be accomplished with the administration of heparin prior to imaging [18]. Hybrid imaging with FDG-PET/magnetic resonance imaging (MRI) has been proposed to assess cardiac sarcoidosis,

representing a combination of two sensitive modalities to assess for myocardial involvement. PET-based methods can help differentiate between acute and post-inflammatory reactions in myocarditis and may also guide endomyocardial biopsies or tailored treatment strategies, such as escalating immunosuppressive therapies during acute exacerbations of inflammation.

Suspected cardiac infections, which are often FDG avid due to inflammatory cell activation, may warrant further evaluation by PET in cases of inconclusive echocardiography [19]. While the sensitivity and specificity of FDG-PET/CT are both high for the diagnosis of prosthetic valve endocarditis, the sensitivity is somewhat lower for native valve endocarditis [20, 21]. High sensitivity and prognostic utility of FDG-PET/CT has been demonstrated in the setting of left ventricular assist device infections [22, 23]. Overall, there is increasing acceptance for clinical use of FDG-PET/CT for the evaluation of infection, and the endorsement of FDG-PET/CT by the European Heart Rhythm Association as a major criterion in the diagnosis of cardiac implantable electronic device infection emphasizes the fact that cardiac infections are not excluded from this trend [24].

Vascular Inflammation

The significance of vascular uptake of FDG as a potential indicator of atherosclerotic disease was first observed by Yun et al. in 2001 [25]. In the context of atherosclerosis, FDG tends to accumulate in macrophages due to their increased glucose utilization that results from activation [26, 27]. The ability to identify clinically relevant atheromas by FDG has been validated by several studies [28, 29]. A study by Ogawa et al. provided the histopathologic evidence that vascular FDG uptake is associated with macrophage infiltration and foam cell formation [26]. The study further showed that FDG uptake was higher when macrophages were actively differentiating into foam cells, rather than in the stage of completely differentiated foam cells.

A strong correlation between FDG-avid lesions and atherosclerotic plaques in different arteries has been observed, including in the aorta, coronary arteries, vertebral arteries, and carotid arteries [6, 29–31]. When Rudd et al. used autoradiography to compare the difference in the FDG uptake between symptomatic and asymptomatic carotid lesions, the authors found that the accumulation of FDG is 27% higher in symptomatic carotid lesions than in contralateral asymptomatic lesions, and no measurable uptake was detected in normal carotid arteries [32]. Studies have shown promising utility of FDG in evaluating the risk of ischemic events [33, 34]. FDG-PET/CT has also shown potential in the ability to assess the effects on medical therapy on the evolution of atheromas [35, 36].

Despite the significant correlation between FDG and atherogenesis as noted by multiple studies, discrepancies have been found between the accumulation of FDG and structural changes detected by the anatomic imaging modalities, especially CT [37, 38]. According to a study by Meirelles et al., disease progression in advanced stages may be accompanied by subdued inflammation, reducing the sensitivity of FDG in such cases [39]. As such, FDG uptake is not generally associated with macro-calcification visible on CT. Results reported by Ben-Haim et al. [40] and Dunphy et al. [37] show only 7% and 2% of cases with CT calcification had corresponding FDG uptake, respectively. In addition to the aforementioned nuances in FDG association with disease activity, the correlation between cardiovascular risk factors and FDG uptake is poorly understood. Risk factors including age, dyslipidemia, smoking history, hypertension, diabetes, etc., are known to play a vital role in the process of atherosclerosis [2]. To date, studies have only been able to successfully prove the clear association between age and FDG avidity [41, 42]. A major limitation of using FDG-PET/CT to assess atherosclerosis is the impracticality of determining disease in the coronary arteries [43]. Expected physiologic uptake of FDG by the myocardium is much higher than the subtle changes in uptake resulting from plaque formation in the coronary arteries. Thus, given the limitations of FDG

in this domain, it is expected that NaF-PET/CT will play a major role in PET-based atherosclerosis imaging [44, 45].

^{18}F-SODIUM FLUORIDE (NAF)

Vascular Micro-calcification

Unlike the nonspecific nature of FDG uptake, NaF localizes specifically to areas of ongoing calcification [46]. Therefore, NaF-PET images are not affected by physiologic myocardial uptake and therefore can detect early signs of coronary plaque micro-calcification in atherosclerosis. Because micro-calcification is mainly composed of inorganic hydroxyapatite, NaF-PET/CT is able to identify thin-cap fibroatheromas, which represent rupture-prone areas (Fig. 2) [47]. NaF was originally introduced as a radiotracer in nuclear medicine by Blau et al. for skeletal imaging given its high uptake by bone [48]; it is therefore important to avoid osseous structures when attempting to quantify vascular uptake of NaF.

NaF-PET has also shown higher sensitivity and specificity than FDG-PET in detecting and characterizing atherosclerosis [49–62]. Furthermore, NaF uptake in atherosclerotic plaque correlates with cardiovascular risk factors but not with coronary calcium scoring [63, 64]. This emphasizes the role of NaF-PET in assessing early rather than late atherosclerotic disease burden. Strong correlations have been found between NaF activity and different cardiovascular risk factors including advancing age, dyslipidemia, diabetes mellitus, and hypertension [65–68]. Moreover, NaF uptake has also been found to be correlated with vital and laboratory values such as blood pressure and the triglycerides-to-high-density lipoprotein ratio [60, 61]. Associations between vascular NaF uptake and cardiovascular scoring systems including Framingham Risk Score (FRS) [69], atherosclerotic cardiovascular disease (ASCVD) risk scores, and CHADS-VASc score have been described as well [70]. However, there is a debate regarding the effect of gender on these correlations [65, 66]. According to McKenney-Drake et al., cardiovascular micro-calcification as shown by NaF-PET/CT has a potential role in risk stratification and the ability to detect arterial calcifications earlier than by CT [49].

In a prospective clinical study by Joshi et al. that compares both FDG and NaF radiotracers, the latter was shown to be superior in identifying culprit lesions from non-culprit lesions among patients with acute coronary syndrome [71]. In another study by Doris et al., it was shown that coronary NaF activity has the ability to provide insight into disease within the coronary circulation by identifying coronary segments with more rapid progression of coronary calcification (Fig. 3) [72]. Kwiecinski et al. found that increased coronary NaF activity is able to serve as a reliable prediction model of both fatal or non-fatal myocardial infarction, independently from age, sex, risk factors, segment involvement, coronary calcium scores, presence of coronary stents, coronary stenosis, REACH, SMART scores, the Duke coronary artery disease index, and recent myocardial infarction [73]. To date, stress testing and conventional coronary angiography can only identify obstructive lesions but do not have the ability to detect high-risk plaques which could potentially cause acute thrombosis. When compared with the high-risk plaque features on intravascular ultrasound (positive remodeling, micro-calcification, and necrosis of the lipid core), Lee et al. demonstrated a significant association with coronary plaques with high focal NaF avidity [74].

The question of quantification of radiotracer activity in an atherosclerotic plaque on PET is difficult given the small size of atheromas and the low resolution of PET [75]. The maximum standardized uptake value (SUVmax) is the most commonly used parameter to measure tracer activity. The use of the target-to-blood pool ratio (TBR) in NaF imaging, a calculation derived by dividing the raw standard uptake value (SUV) to the venous blood pool SUV remains controversial [30]. Global assessment with NaF-PET/CT could potentially overcome the difficulty in quantifying atherosclerotic plaques by defining a region of interest that encompasses the entire affected vessel [43, 76].

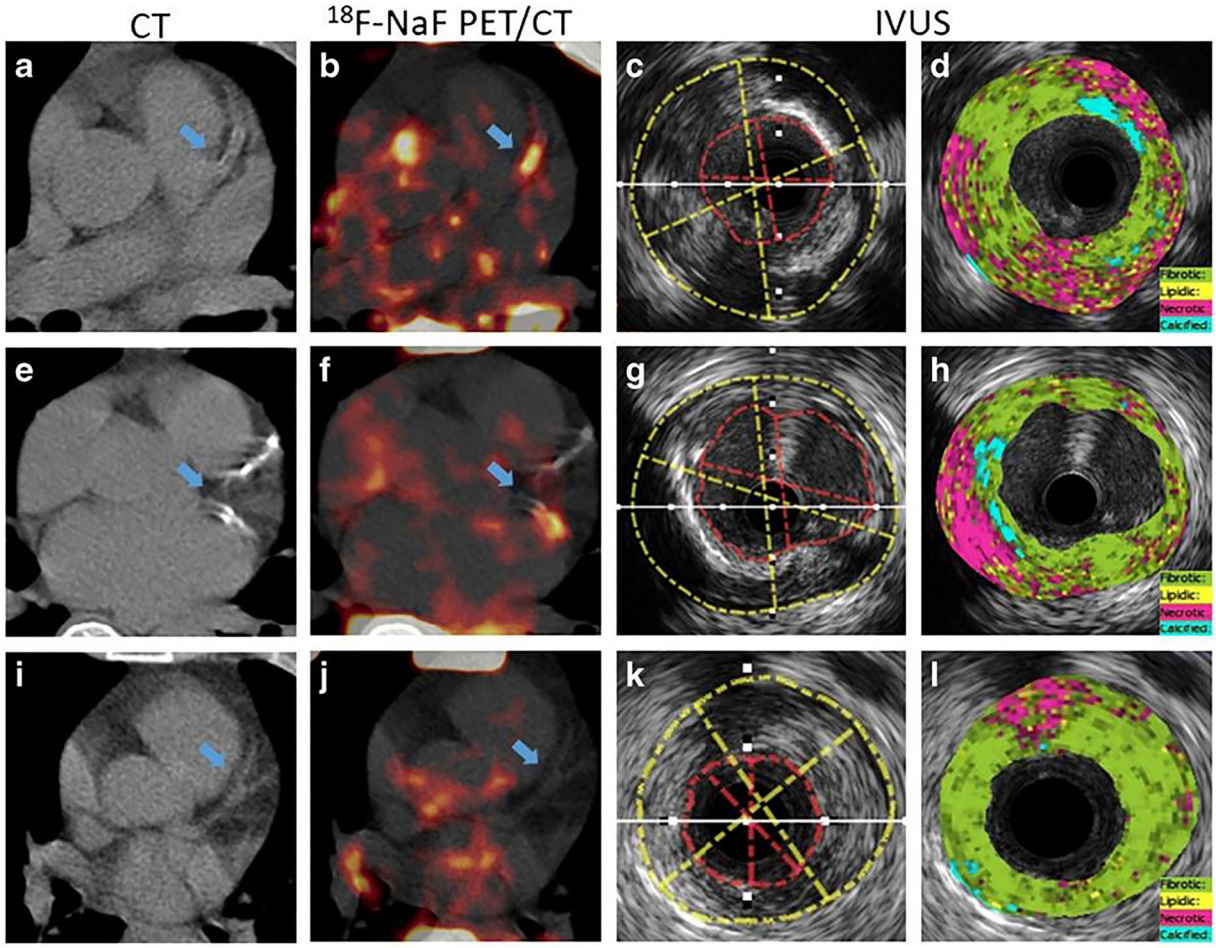

Fig. 2 CT, fused NaF-PET/CT, and IVUS images from three patients with unstable angina. While lesions with spotty calcification (**a–d**) and a large necrotic core (**e–h**) were NaF avid, the fibrotic lesion (**i–l**) did not demonstrate focal uptake. Image reprinted without changes from Li et al. [47] under the Creative Commons Attribution 4.0 International License (CC BY). https://creativecommons.org/licenses/by/4.0/

Valvular Calcification

Calcification is a major mechanism causing aortic stenosis [77], the most frequent form of valvular heart disease in the Western world [78]. On CT, the degree of calcification of the aortic valve can be determined quantitatively and precisely, and it appears to correspond with the hemodynamic severity of the aortic stenosis [79, 80]. Hence, the ESC/EACTS Guidelines on Valvular Heart Disease suggest that CT calcium scoring should be used as a first-line test in cases with discordant grading [81]. However, NaF-PET/CT imaging has the advantage of being able to determine the degree by which active calcification is occurring [82]. In addition, histological markers of calcification activity coincide with NaF [83]. Thus, patients with more severe disease have the highest degree of tracer uptake [12], explaining why disease progression is faster in patients with severe AS. New calcification could be identified in the areas of elevated NaF activity reported on the baseline scan if patients undergo repeat CT calcium scoring [83]. As a result, baseline NaF uptake can predict disease progression and related adverse cardiovascular events. Hence, it might also be used to assess the effects of novel drugs on disease activity

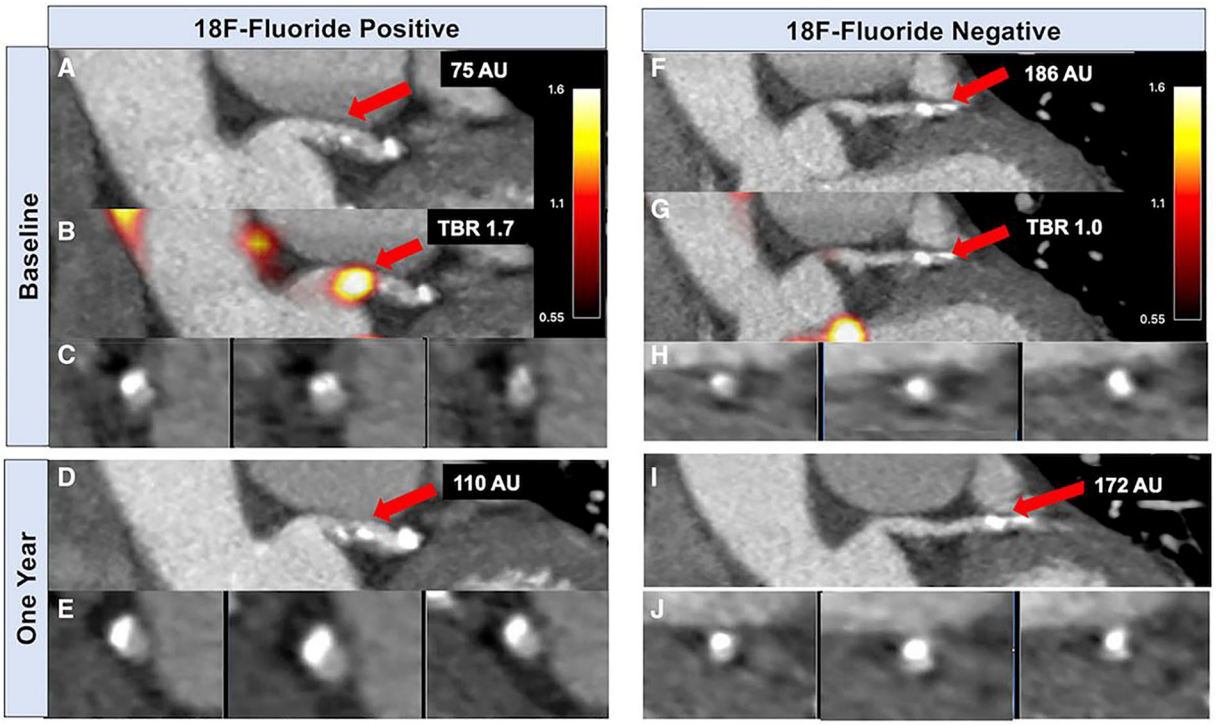

Fig. 3 Baseline and repeat imaging of two coronary plaques in the same patient. Contrast-enhanced CT coronary angiography (**A**, **C**) and fused PET/CT (**B**) demonstrate NaF activity localized to calcification present in the left main stem. CT coronary angiography 1 year later (**D**, **E**) demonstrates increased CT calcification at this site. By contrast, CT coronary angiography (**F**, **H**) and PET/CT (**G**) showed a non-NaF avid calcified plaque in a proximal obtuse marginal branch, which was not found to have increased calcification after 1 year (**I**, **J**). Image reprinted without changes from Doris et al. [72] under the Creative Commons Attribution 4.0 International License (CC BY). https://creativecommons.org/licenses/by/4.0/

besides assessing the durability of transcatheter aortic valve replacements. Additionally, PET/MRI offers simultaneous imaging of calcification activity in the aortic valve using NaF in addition to detailed assessment of markers of myocardial decompensation. Hence, further testing for signs of calcification in bioprosthetic valves as an early marker of valve degradation using PET/MRI may be possible.

Cardiac Amyloidosis

The two types of cardiac amyloidosis are acquired monoclonal immunoglobulin light-chain (AL) and transthyretin-related (familial and wild-type/senile) amyloidosis (ATTR). CMR is routinely used in the assessment of cardiac amyloidosis. However, CMR is unable to differentiate between AL and ATTR amyloidosis. Because there is higher NaF activity in ATTR cardiac amyloidosis but not AL amyloidosis, NaF-PET/CT may be a viable non-invasive method to discriminate ATTR from AL [84]. This variation in tracer uptake shows that the kind of amyloid deposits in the myocardium influences calcium homeostasis locally. In patients with ATTR amyloidosis, NaF uptake could be effective for disease monitoring and amyloid deposition localization [85].

In addition to NaF, PET tracers which target amyloid fibrils, including ^{11}C-Pittsburgh compound B (^{11}C-PiB), ^{18}F-florbetaben, ^{18}F-florbetapir, and ^{18}F-flutemetamol, have been proposed to image cardiac amyloidosis [86]. A study by Park et al. utilizing autoradiography suggested that ^{18}F-florbetapir binds AL to a higher degree than to ATTR [87]. A similar

pattern of differential uptake among cardiac amyloidosis subtypes has been described using ^{18}F-florbetaben [88]. A meta-analysis by Kim et al. reported high sensitivity and specificity of amyloid PET in the diagnosis of cardiac amyloidosis, suggesting that amyloid PET imaging may play an additional role in identifying amyloid subtypes [89].

OTHER RADIOTRACERS

Myocardial Perfusion Imaging

^{82}Rb is a radiotracer that is absorbed from the blood by the myocardium via the Na^+/K^+-ATPase [90]. It has been widely utilized with PET and has become an important technique for determining myocardial blood flow and coronary reserve (Fig. 4) [91, 92]. As such, it is widely accepted as a standard for coronary artery disease imaging [93]. In a recent prospective study done by Gaudieri et al. on 517 hypertensive subjects of which 26% had resistant hypertension, ^{82}Rb-PET was able to perform risk stratification by assessing coronary vascular function [94]. According to the authors, subjects with resistant hypertension and coronary vascular dysfunction have the highest risk of cardiovascular events. However, the practical usage of ^{82}Rb-PET is limited by a short half-life and a long positron range. Other PET tracers proposed for perfusion imaging suffer from similar technical concerns which limit their widespread adoption. For example, ^{15}O-water produces images with a low signal-to-noise ratio, and ^{13}N-ammonia still has a longer positron range compared to ^{18}F-labeled tracers [95, 96].

^{18}F-flupiridaz is a pyridazinone derivative that targets the mitochondrial complex I of the electron transport chain with high affinity. The method of localization for this radiotracer is deemed cardioselective because mitochondria make up roughly 20–30% of the cellular volume of the myocardium, resulting in higher myocardial uptake compared to the lungs and liver [97]. ^{18}F-flurpiridaz has shown to be advantageous in detecting myocardial blood flow [98]. It has demonstrated a high level of uptake in the heart, and it has a high myocardial extraction fraction, permitting easier quantification using PET [99]. Myocardial perfusion imaging with ^{18}F-flurpiridaz-PET was found to have superior diagnostic ability compared to ^{99m}Tc-labeled SPECT in women, obese individuals, and those undergoing pharmacological stress testing in a phase III clinical trial [100]. Therefore, abnormalities in myocardial perfusion may be assessed by ^{18}F-flupiridaz, which has the potential to become a routine clinical test.

^{18}F-Flubrobenguane

^{18}F-flubrobenguane, also referred to as ^{18}F-LMI1195, is a ^{18}F-labeled norepinephrine (NE) transporter ligand demonstrating clinical promise for its ability to evaluate cardiac sympathetic function as a PET radiotracer [101]. ^{11}C-metahydroxyephedrine (^{11}C-HED) is a NE transporter ligand PET tracer similar to ^{18}F-flubrobenguane but has limited use due to its short half-life. Uptake of ^{18}F-flubrobenguane has been shown to closely mimic the physiologic NE uptake mechanism, thereby allowing for evaluation of cardiac neuronal integrity and function. Physiologic NE is stored in presynaptic vesicles and released upon neural impulse into the synaptic cleft via vesicular exocytosis. At the post-synaptic cleft, adrenoreceptors are activated. NE is then transported to the presynaptic cleft for reuptake and is stored before the next firing impulse. It has been demonstrated that blockage of the NE transporter via a selective NE transporter inhibitor, desipramine, reduces uptake of ^{18}F-flubrobenguane considerably, suggesting that ^{18}F-flubrobenguane closely mimics NE turnover [102]. Furthermore, early data have shown that ^{18}F-flubrobenguane provides a well-tolerated non-invasive assessment of cardiac regional denervation and heterogeneity of innervation [103].

PET imaging with ^{18}F-flubrobenguane allows for evaluation of damage to the cardiac nervous system, thereby identifying individuals at high risk for cardiac events. For example, heart failure has been associated with increased sympathetic activity within the heart. This increase in NE release downregulates the NE transporter

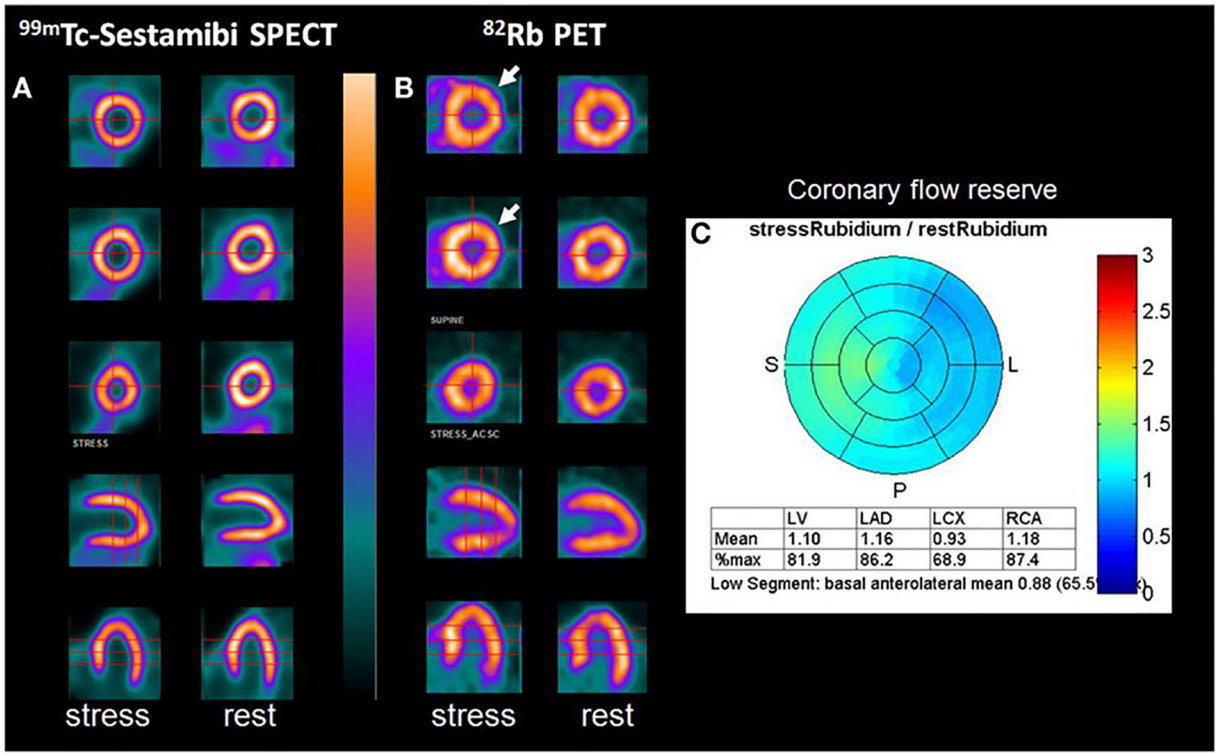

Fig. 4 ^{99m}Tc-sestamibi SPECT (**A**) and ^{82}Rb-PET/CT (**B**) studies performed in a 56-year-old woman. Ischemia involving the circumflex artery (*arrow*) was evident by ^{82}Rb-PET after administration of dipyridamole, demonstrating the superior sensitivity of this technique. Image reprinted without changes from Chatal et al. [92] under the Creative Commons Attribution 4.0 International License (CC BY). https://creativecommons.org/licenses/by/4.0/

responsible for its reuptake, thereby increasing synaptic concentrations of NE. Higher concentrations of NE desensitize beta-adrenoceptors, which would otherwise slow progression of cardiac disease [104]. Since regional cardiac sympathetic dysfunction has been associated with incidence of ventricular arrhythmias and sudden cardiac death (SCD), PET can be used to guide management and stage patients for implantable cardioverter-defibrillator placement [105]. In the Prediction of ARrhythmic Events with PET (PAREPET) trial, patients were imaged with echocardiography, ^{11}C-HED PET, ^{13}N-ammonia PET for perfusion, and FDG-PET for viability to assess predictors of SCD [106]. Results from the PAREPET trial showed that sympathetic denervation imaged by ^{11}C-HED PET could predict cause-specific SCD [107]. A later analysis showed that regional rather than global parameters derived from ^{11}C-HED PET were superior in determining SCD risk [108]. The PAREPET II trial aims to evaluate the role of ^{18}F-flubrobenguane in characterizing left ventricular sympathetic denervation, with SCD serving as the primary endpoint [109]. The results of this ongoing trial may clarify the role of imaging sympathetic function by PET in determining which patients would benefit from an implantable cardioverter-defibrillator.

CONCLUSIONS

Early detection of atherogenesis with FDG and NaF represents an exciting development within cardiac PET. Furthermore, evaluation of inflammation and ATTR amyloid deposition affecting the myocardium can be detected with FDG and NaF, respectively. Cardiac sarcoidosis in particular is a domain that can benefit from

the additional characterization only available by FDG-PET. A large number of additional tracers, both in constant routine use as well as newly introduced, are under investigation into their utility in assessing the consequences of ischemic cardiomyopathy. As future studies provide further validation for these tracers and clarify their optimal usages, it is expected that patient care and our scientific understanding of CVD will continue to benefit from the knowledge provided by cardiac PET imaging.

ACKNOWLEDGEMENTS

Funding. No funding or sponsorship was received for this study or publication of this article.

Author Contributions. Conceptualization, S.B.S. and W.Y.R.; writing—original draft preparation, S.B.S., S.J.N., H.C.L., K.K., S.B., P.P., B.B.S., R.N., S.S., S.G., and W.Y.R.; writing—review and editing, S.J.N., H.C.L., and W.Y.R. All authors have read and agreed to the published version of the manuscript.

Disclosures. Shashi Bhushan Singh, Sze Jia Ng, Hui Chong Lau, Kishor Khanal, Sanket Bhattarai, Pranita Paudyal, Bimash Babu Shrestha, Rizwan Naseer, Simran Sandhu, Saket Gokhale and William Y. Raynor have nothing to disclose.

Compliance with Ethics Guidelines. This article is based on previously conducted studies and does not contain any new studies with human participants or animals performed by any of the authors.

Data Availability. Data sharing is not applicable to this article as no datasets were generated or analyzed during the current study.

REFERENCES

1. Virani SS, et al. Heart disease and stroke statistics—2020 update: a report from the American Heart Association. Circulation. 2020;141(9).
2. Gimbrone MA, García-Cardeña G. Endothelial cell dysfunction and the pathobiology of atherosclerosis. Circ Res. 2016;118(4):620–36.
3. Libby P. Inflammation in atherosclerosis. Nature. 2002;420(6917):868–74.
4. Osborn EA, Jaffer FA. Imaging atherosclerosis and risk of plaque rupture. Curr Atheroscler Rep. 2013;15(10).
5. Syed MB, et al. Emerging techniques in atherosclerosis imaging. Br J Radiol. 2019;92(1103):20180309.
6. Mayer M, et al. Imaging atherosclerosis by PET, with emphasis on the role of FDG and NaF as potential biomarkers for this disorder. Front Physiol. 2020;11:511391.
7. McKenney-Drake ML, et al. (18)F-NaF PET imaging of early coronary artery calcification. JACC Cardiovasc Imaging. 2016;9(5):627–8.
8. McKenney-Drake ML, et al. (18)F-NaF and (18)F-FDG as molecular probes in the evaluation of atherosclerosis. Eur J Nucl Med Mol Imaging. 2018;45(12):2190–200.
9. Hancin EC, et al. Non-(18)F-FDG/(18)F-NaF radiotracers proposed for the diagnosis and management of diseases of the heart and vasculature. PET Clin. 2021;16(2):273–84.

10. Khalaf S, Al-Mallah MH. Fluorodeoxyglucose applications in cardiac PET: viability, inflammation, infection, and beyond. Methodist Debakey Cardiovasc J. 2020;16(2):122–9.

11. Rojulpote C, et al. Role of FDG-PET/CT in assessing the correlation between blood pressure and myocardial metabolic uptake. Asia Ocean J Nucl Med Biol. 2020;8(1):36–45.

12. Tillisch J, et al. Reversibility of cardiac wall-motion abnormalities predicted by positron tomography. N Engl J Med. 1986;314(14):884–8.

13. Ghosh N, et al. Assessment of myocardial ischaemia and viability: role of positron emission tomography. Eur Heart J. 2010;31(24):2984–95.

14. Manabe O, et al. Multimodality evaluation of cardiac sarcoidosis. J Nucl Cardiol. 2012;19(3):621–4.

15. Christopoulos G, et al. Suppressing physiologic 18-fluorodeoxyglucose uptake in patients undergoing positron emission tomography for cardiac sarcoidosis: the effect of a structured patient preparation protocol. J Nucl Cardiol. 2021;28(2):661–71.

16. Atterton-Evans V, et al. Variances of dietary preparation for suppression of physiological (18)F-FDG myocardial uptake in the presence of cardiac sarcoidosis: a systematic review. J Nucl Cardiol. 2020;27(2):481–9.

17. Ozutemiz C, et al. Comparison of the effect of three different dietary modifications on myocardial suppression in (18)F-FDG PET/CT evaluation of patients for suspected cardiac sarcoidosis. J Nucl Med. 2021;62(12):1759–67.

18. Scholtens AM, et al. Suppression of myocardial glucose metabolism in FDG PET/CT: impact of dose variation in heparin bolus pre-administration. Eur J Nucl Med Mol Imaging. 2020;47(11):2698–702.

19. Dilsizian V, et al. Best practices for imaging cardiac device-related infections and endocarditis: a JACC: cardiovascular imaging expert panel statement. JACC Cardiovasc Imaging. 2022;15(5):891–911.

20. Gomes A, et al. Imaging infective endocarditis: Adherence to a diagnostic flowchart and direct comparison of imaging techniques. J Nucl Cardiol. 2020;27(2):592–608.

21. de Camargo RA, et al. The role of 18F-fluorodeoxyglucose positron emission tomography/computed tomography in the diagnosis of left-sided endocarditis: native vs prosthetic valves endocarditis. Clin Infect Dis. 2020;70(4):583–94.

22. Sommerlath Sohns JM, et al. (18)F-FDG PET/CT in left-ventricular assist device infection: initial results supporting the usefulness of image-guided therapy. J Nucl Med. 2020;61(7):971–6.

23. Tam MC, et al. Diagnostic accuracy of FDG PET/CT in suspected LVAD infections: a case series, systematic review, and meta-analysis. JACC Cardiovasc Imaging. 2020;13(5):1191–202.

24. Blomstrom-Lundqvist C, et al. European Heart Rhythm Association (EHRA) international consensus document on how to prevent, diagnose, and treat cardiac implantable electronic device infections-endorsed by the Heart Rhythm Society (HRS), the Asia Pacific Heart Rhythm Society (APHRS), the Latin American Heart Rhythm Society (LAHRS), International Society for Cardiovascular Infectious Diseases (ISCVID) and the European Society of Clinical Microbiology and Infectious Diseases (ESCMID) in collaboration with the European Association for Cardio-Thoracic Surgery (EACTS). Europace. 2020;22(4):515–49.

25. Yun M, et al. F-18 FDG uptake in the large arteries: a new observation. Clin Nucl Med. 2001;26(4):314–9.

26. Ogawa M, et al. What can be seen by ^{18}F-FDG PET in atherosclerosis imaging? The effect of foam cell formation on ^{18}F-FDG uptake to macrophages in vitro. J Nucl Med. 2012;53(1):55–8.

27. Moghbel M, et al. The role of PET in evaluating atherosclerosis: a critical review. Semin Nucl Med. 2018;48(6):488–97.

28. Pasha AK, et al. Effects of age and cardiovascular risk factors on (18)F-FDG PET/CT quantification of atherosclerosis in the aorta and peripheral arteries. Hell J Nucl Med. 2015;18(1):5–10.

29. Davies JR, et al. Identification of culprit lesions after transient ischemic attack by combined ^{18}F fluorodeoxyglucose positron-emission tomography and high-resolution magnetic resonance imaging. Stroke. 2005;36(12):2642–7.

30. Tawakol A, et al. In vivo 18F-fluorodeoxyglucose positron emission tomography imaging provides a noninvasive measure of carotid plaque inflammation in patients. J Am Coll Cardiol. 2006;48(9):1818–24.

31. Graebe M, et al. Molecular pathology in vulnerable carotid plaques: correlation with [18]-fluorodeoxyglucose positron emission tomography (FDG-PET). Eur J Vasc Endovasc Surg. 2009;37(6):714–21.

32. Rudd JHF, et al. Imaging atherosclerotic plaque inflammation with ^{18}F-fluorodeoxyglucose positron

emission tomography. Circulation. 2002;105(23):2708–11.

33. Figueroa AL, et al. Distribution of inflammation within carotid atherosclerotic plaques with high-risk morphological features. Circ Cardiovasc Imaging. 2012;5(1):69–77.

34. Marnane M, et al. Carotid plaque inflammation on 18F-fluorodeoxyglucose positron emission tomography predicts early stroke recurrence. Ann Neurol. 2012;71(5):709–18.

35. Tahara N, et al. Simvastatin attenuates plaque inflammation: evaluation by fluorodeoxyglucose positron emission tomography. J Am Coll Cardiol. 2006;48(9):1825–31.

36. Ogawa M, et al. Application of 18F-FDG PET for monitoring the therapeutic effect of antiinflammatory drugs on stabilization of vulnerable atherosclerotic plaques. J Nucl Med. 2006;47(11):1845–50.

37. Dunphy MP, et al. Association of vascular 18F-FDG uptake with vascular calcification. J Nucl Med. 2005;46(8):1278–84.

38. Tatsumi M, et al. Fluorodeoxyglucose uptake in the aortic wall at PET/CT: possible finding for active atherosclerosis. Radiology. 2003;229(3):831–7.

39. Meirelles GS, Gonen M, Strauss HW. 18F-FDG uptake and calcifications in the thoracic aorta on positron emission tomography/computed tomography examinations: frequency and stability on serial scans. J Thorac Imaging. 2011;26(1):54–62.

40. Ben-Haim S, et al. Evaluation of 18F-FDG uptake and arterial wall calcifications using 18F-FDG PET/CT. J Nucl Med. 2004;45(11):1816–21.

41. Yun M, et al. 18F FDG uptake in the large arteries: a correlation study with the atherogenic risk factors. Semin Nucl Med. 2002;32(1):70–6.

42. Bural GG, et al. FDG-PET is an effective imaging modality to detect and quantify age-related atherosclerosis in large arteries. Eur J Nucl Med Mol Imaging. 2008;35(3):562–9.

43. Alavi A, Werner TJ, Høilund-Carlsen PF. What can be and what cannot be accomplished with PET to detect and characterize atherosclerotic plaques. J Nucl Cardiol. 2018;25(6):2012–5.

44. Raynor WY, et al. PET-based imaging with (18)F-FDG and (18)F-NaF to assess inflammation and microcalcification in atherosclerosis and other vascular and thrombotic disorders. Diagnostics (Basel). 2021;11(12).

45. Alavi A, et al. Critical review of PET imaging for detection and characterization of the atherosclerotic plaques with emphasis on limitations of FDG-PET compared to NaF-PET in this setting. Am J Nucl Med Mol Imaging. 2021;11(5):337–51.

46. Raynor WY, et al. Novel musculoskeletal and orthopedic applications of (18)F-sodium fluoride PET. PET Clin. 2021;16(2):295–311.

47. Li L, et al. Sodium-fluoride PET-CT for the non-invasive evaluation of coronary plaques in symptomatic patients with coronary artery disease: a cross-correlation study with intravascular ultrasound. Eur J Nucl Med Mol Imaging. 2018;45(12):2181–9.

48. Blau M, Nagler W, Bender MA. Fluorine-18: a new isotope for bone scanning. J Nucl Med. 1962;3:332–4.

49. McKenney-Drake ML, et al. 18F-NaF and 18F-FDG as molecular probes in the evaluation of atherosclerosis. Eur J Nucl Med Mol Imaging. 2018;45(12):2190–200.

50. Blomberg BA, et al. Reference values for fluorine-18-fluorodeoxyglucose and fluorine-18-sodium fluoride uptake in human arteries: a prospective evaluation of 89 healthy adults. Nucl Med Commun. 2017;38(11):998–1006.

51. Blomberg BA, et al. Thoracic aorta calcification but not inflammation is associated with increased cardiovascular disease risk: results of the CAMONA study. Eur J Nucl Med Mol Imaging. 2017;44(2):249–58.

52. Fujimoto K, et al. Association between carotid 18F-NaF and 18F-FDG uptake on PET/CT with ischemic vascular brain disease on MRI in patients with carotid artery disease. Ann Nucl Med. 2019;33(12):907–15.

53. Guaraldi G, et al. 18Fluoride-based molecular imaging of coronary atherosclerosis in HIV infected patients. Atherosclerosis. 2020;297:127–35.

54. Raynor W, et al. Evolving role of molecular imaging with (18)F-sodium fluoride PET as a biomarker for calcium metabolism. Curr Osteoporos Rep. 2016;14(4):115–25.

55. Hoilund-Carlsen PF, et al. Atherosclerosis imaging with (18)F-sodium fluoride PET. Diagnostics (Basel). 2020;10(10).

56. Raynor WY, et al. (18)F-sodium fluoride: an emerging tracer to assess active vascular microcalcification. J Nucl Cardiol. 2021;28(6):2706–11.

57. Gonuguntla K, et al. Utilization of NaF-PET/CT in assessing global cardiovascular calcification using CHADS2 and CHADS2-VASc scoring systems in high risk individuals for cardiovascular disease. Am J Nucl Med Mol Imaging. 2020;10(6):293–300.

58. Castro SA, et al. Carotid artery molecular calcification assessed by [(18)F]fluoride PET/CT: correlation with cardiovascular and thromboembolic risk factors. Eur Radiol. 2021;31(10):8050–9.

59. Seraj SM, et al. Assessing the feasibility of NaF-PET/CT versus FDG-PET/CT to detect abdominal aortic calcification or inflammation in rheumatoid arthritis patients. Ann Nucl Med. 2020;34(6):424–31.

60. Rojulpote C, et al. NaF-PET/CT global assessment in detecting and quantifying subclinical cardiac atherosclerosis and its association with blood pressure in non-dyslipidemic individuals. Am J Cardiovasc Dis. 2020;10(2):101–7.

61. Patil S, et al. Association of triglyceride to high density lipoprotein ratio with global cardiac microcalcification to evaluate subclinical coronary atherosclerosis in non-diabetic individuals. Am J Cardiovasc Dis. 2020;10(3):241–6.

62. Bhattaru A, et al. An understanding of the atherosclerotic molecular calcific heterogeneity between coronary, upper limb, abdominal, and lower extremity arteries as assessed by NaF PET/CT. Am J Nucl Med Mol Imaging. 2021;11(1):40–5.

63. Fiz F, et al. 18F-NaF uptake by atherosclerotic plaque on PET/CT imaging: inverse correlation between calcification density and mineral metabolic activity. J Nucl Med. 2015;56(7):1019–23.

64. de Oliveira-Santos M, et al. Atherosclerotic plaque metabolism in high cardiovascular risk subjects—a subclinical atherosclerosis imaging study with 18F-NaF PET-CT. Atherosclerosis. 2017;260:41–6.

65. Blomberg BA, et al. Coronary fluorine-18-sodium fluoride uptake is increased in healthy adults with an unfavorable cardiovascular risk profile: results from the CAMONA study. Nucl Med Commun. 2017;38(11):1007–14.

66. Derlin T, et al. In vivo imaging of mineral deposition in carotid plaque using ^{18}F-sodium fluoride PET/CT: correlation with atherogenic risk factors. J Nucl Med. 2011;52(3):362–8.

67. Beheshti M, et al. Detection and global quantification of cardiovascular molecular calcification by fluoro18-fluoride positron emission tomography/computed tomography—a novel concept. Hell J Nucl Med. 2011;14(2):114–20.

68. Janssen T, et al. Association of linear 18F-sodium fluoride accumulation in femoral arteries as a measure of diffuse calcification with cardiovascular risk factors: a PET/CT study. J Nucl Cardiol. 2013;20(4):569–77.

69. Morbelli S, et al. Divergent determinants of 18F-NaF uptake and visible calcium deposition in large arteries: relationship with Framingham risk score. Int J Cardiovasc Imaging. 2014;30(2):439–47.

70. Gonuguntla K, et al. Utilization of NaF-PET/CT in assessing global cardiovascular calcification using CHADS(2) and CHADS(2)-VASc scoring systems in high risk individuals for cardiovascular disease. Am J Nucl Med Mol Imaging. 2020;10(6):293–300.

71. Joshi NV, et al. 18F-fluoride positron emission tomography for identification of ruptured and high-risk coronary atherosclerotic plaques: a prospective clinical trial. Lancet. 2014;383(9918):705–13.

72. Doris MK, et al. Coronary (18)F-fluoride uptake and progression of coronary artery calcification. Circ Cardiovasc Imaging. 2020;13(12): e011438.

73. Kwiecinski J, et al. Coronary (18)F-sodium fluoride uptake predicts outcomes in patients with coronary artery disease. J Am Coll Cardiol. 2020;75(24):3061–74.

74. Lee JM, et al. Clinical relevance of ^{18}F-sodium fluoride positron-emission tomography in noninvasive identification of high-risk plaque in patients with coronary artery disease. Circ Cardiovasc Imaging. 2017;10(11).

75. Alavi A, Werner TJ, Hoilund-Carlsen PF. What can be and what cannot be accomplished with PET to detect and characterize atherosclerotic plaques. J Nucl Cardiol. 2018;25(6):2012–5.

76. Saboury B, et al. Alavi-Carlsen Calcification Score (ACCS): a simple measure of global cardiac atherosclerosis burden. Diagnostics (Basel), 2021;11(8).

77. Pawade TA, Newby DE, Dweck MR. Calcification in aortic stenosis: the skeleton key. J Am Coll Cardiol. 2015;66(5):561–77.

78. Iung B, et al. A prospective survey of patients with valvular heart disease in Europe: The Euro Heart Survey on Valvular Heart Disease. Eur Heart J. 2003;24(13):1231–43.

79. Cueff C, et al. Measurement of aortic valve calcification using multislice computed tomography: correlation with haemodynamic severity of aortic stenosis and clinical implication for patients with low ejection fraction. Heart. 2011;97(9):721–6.

80. Pawade T, et al. Computed tomography aortic valve calcium scoring in patients with aortic stenosis. Circ Cardiovasc Imaging. 2018;11(3):e007146.

81. Baumgartner H, et al. 2017 ESC/EACTS Guidelines for the management of valvular heart disease. Kardiologia Polska (Polish Heart Journal). 2018;76(1): 1–62.

82. Rojulpote C, et al. Role of (18)F-NaF-PET in assessing aortic valve calcification with age. Am J Nucl Med Mol Imaging. 2020;10(1):47–56.

83. Dweck MR, et al. 18F-sodium fluoride uptake is a marker of active calcification and disease progression in patients with aortic stenosis. Circ Cardiovasc Imaging. 2014;7(2):371–8.

84. Trivieri MG, et al. 18F-sodium fluoride PET/MR for the assessment of cardiac amyloidosis. J Am Coll Cardiol. 2016;68(24):2712–4.

85. Morgenstern R, et al. 18Fluorine sodium fluoride positron emission tomography, a potential biomarker of transthyretin cardiac amyloidosis. J Nucl Cardiol. 2018;25(5):1559–67.

86. Slart R, et al. Procedural recommendations of cardiac PET/CT imaging: standardization in inflammatory-, infective-, infiltrative-, and innervation-(4Is) related cardiovascular diseases: a joint collaboration of the EACVI and the EANM: summary. Eur Heart J Cardiovasc Imaging. 2020;21(12):1320–30.

87. Park MA, et al. 18F-florbetapir binds specifically to myocardial light chain and transthyretin amyloid deposits: autoradiography study. Circ Cardiovasc Imaging. 2015;8(8).

88. Kircher M, et al. Detection of cardiac amyloidosis with (18)F-Florbetaben-PET/CT in comparison to echocardiography, cardiac MRI and DPD-scintigraphy. Eur J Nucl Med Mol Imaging. 2019;46(7): 1407–16.

89. Kim YJ, Ha S, Kim YI. Cardiac amyloidosis imaging with amyloid positron emission tomography: a systematic review and meta-analysis. J Nucl Cardiol. 2020;27(1):123–32.

90. Huang S-C, et al. Rabbit myocardial 82Rb kinetics and a compartmental model for blood flow estimation. Am J Physiol Heart Circul Physiol. 1989;256(4):H1156–64.

91. Chatal J-F, et al. Story of rubidium-82 and advantages for myocardial perfusion PET imaging. Front Med. 2015;2:65.

92. Chatal JF, et al. Story of rubidium-82 and advantages for myocardial perfusion PET imaging. Front Med (Lausanne). 2015;2:65.

93. Renaud JM, et al. Clinical interpretation standards and quality assurance for the multicenter PET/CT trial rubidium-ARMI. J Nucl Med. 2014;55(1):58–64.

94. Gaudieri V, et al. Prognostic value of coronary vascular dysfunction assessed by rubidium-82 PET/CT imaging in patients with resistant hypertension without overt coronary artery disease. Eur J Nucl Med Mol Imaging. 2021;48(10):3162–71.

95. Werner RA, et al. Moving into the next era of PET myocardial perfusion imaging: introduction of novel (18)F-labeled tracers. Int J Cardiovasc Imaging. 2019;35(3):569–77.

96. Li Y, et al. Advanced tracers in PET imaging of cardiovascular disease. Biomed Res Int. 2014;2014: 504532.

97. Huisman MC, et al. Initial characterization of an 18F-labeled myocardial perfusion tracer. J Nucl Med. 2008;49(4):630–6.

98. Calnon DA. Will 18F flurpiridaz replace 82rubidium as the most commonly used perfusion tracer for PET myocardial perfusion imaging? Springer; 2019. pp. 2031–2033.

99. Moody JB, et al. Added value of myocardial blood flow using 18F-flurpiridaz PET to diagnose coronary artery disease: the flurpiridaz 301 trial. J Nucl Cardiol. 2021;28(5):2313–29.

100. Maddahi J, et al. Phase-III clinical trial of fluorine-18 flurpiridaz positron emission tomography for evaluation of coronary artery disease. J Am Coll Cardiol. 2020;76(4):391–401.

101. Werner RA, et al. Recent paradigm shifts in molecular cardiac imaging-establishing precision cardiology through novel (18)F-labeled PET radiotracers. Trends Cardiovasc Med. 2020;30(1):11–9.

102. Werner RA, et al. Retention kinetics of the 18F-labeled sympathetic nerve PET tracer LMI1195: comparison with 11C-hydroxyephedrine and 123I-MIBG. J Nucl Med. 2015;56(9):1429–33.

103. Sinusas AJ, et al. Biodistribution and radiation dosimetry of LMI1195: first-in-human study of a novel 18F-labeled tracer for imaging myocardial innervation. J Nucl Med. 2014;55(9):1445–51.

104. Yu M, et al. Evaluation of LMI1195, a novel 18F-labeled cardiac neuronal PET imaging agent, in cells and animal models. Circ Cardiovasc Imaging. 2011;4(4):435–43.

105. Yu M, et al. LMI1195 PET imaging in evaluation of regional cardiac sympathetic denervation and its potential role in antiarrhythmic drug treatment. Eur J Nucl Med Mol Imaging. 2012;39(12):1910–9.

106. Fallavollita JA, et al. Prediction of arrhythmic events with positron emission tomography: PAREPET study design and methods. Contemp Clin Trials. 2006;27(4):374–88.

107. Fallavollita JA, et al. Regional myocardial sympathetic denervation predicts the risk of sudden cardiac arrest in ischemic cardiomyopathy. J Am Coll Cardiol. 2014;63(2):141–9.

108. Zelt JGE, et al. Positron emission tomography imaging of regional versus global myocardial sympathetic activity to improve risk stratification in patients with ischemic cardiomyopathy. Circ Cardiovasc Imaging. 2021;14(6): e012549.

109. van der Bijl P, et al. Cardiac sympathetic innervation imaging with PET radiotracers. Curr Cardiol Rep. 2020;23(1):4.